Bull. Chem. Soc. Jpn., 74, 2091–2099 (2001)

Comparative Structural, Spectroscopic and Redox Studies of Isostructural Complexes of Ruthenium(III), Osmium(III), and Rhenium(III): *cis*-Dichloro Complexes Containing Tris(2-pyridylmethyl)amine and Its 6-Methylpyridyl Derivative

Hideki Sugimoto,* Chikako Matsunami,† Chikako Koshi,† Mikio Yamasaki,†† Keisuke Umakoshi,†,# and Yoichi Sasaki*,†

Department of Chemistry, Graduate School of Science, Osaka City University, Sugimoto, Sumiyoshi-ku,
Osaka 558-8585

†Division of Chemistry, Graduate School of Science, Hokkaido University, Kita-ku, Sapporo 060-0810

††Rigaku Corporation, Matsubara, Akishima, Tokyo 196-8666

(Received April 27, 2001)

A series of the complexes, $[MCl_2(L)]^+$ (M = Ru, L = tpa (**1**), Metpa (**1a**); M = Os, L = tpa (**2**); M = Re, L = tpa (**3**), Metpa (**3a**); tpa = tris(2-pyridylmethyl)amine, Metpa = ((6-methyl-2-pyridylmethyl)bis(2-pyridylmethyl)amine), have been prepared. X-ray structural analyses of the series of isostructural complexes [**1a**]BF_4, [**2**]$PF_6{\cdot}C_2H_5OC_2H_5$, [**3**]BF_4, and [**3a**]BF_4 together with that of the previously reported [**1**]ClO_4, made detailed comparison of structure parameters for Ru, Os, and Re possible. The corresponding metal-ligand bond lengths which are similar between [**1**]ClO_4 and [**2**]$PF_6{\cdot}C_2H_5OC_2H_5$ are considerably longer (0.02–0.03 Å) for [**3**]BF_4, especially in the case of M–N(tertially nitrogen) (0.06 Å) bond. The M–Cl(trans to tertially nitrogen) bond lengths do not follow this trend. Introduction of the methyl group causes significant influence on the structure of the Re(III) complex: increase in bond length of Re–N(methylated pyridyl) and Re–N(pyridyl) trans to it. Bond angles around the metal ion related to the methylated pyridyl group are also significantly affected. Such steric influence is not clear for [**1a**]BF_4 due to disorder of methyl group. The redox waves of the two processes, M(II/III) and M(III/IV), are observed for all the complexes. The redox potentials for individual process follow the order: Ru $<$ Os $<$ Re (from negative to positive), the difference being ca. 0.5 V. The difference in the two consecutive redox potentials is almost identical (ca. 1.6 V) among the three metal ions, suggesting that the stabilities of the trivalent oxidation state over di- and tetravalent ones are not affected by the different d-electron configurations. Strong visible MLCT bands are observed only for the rhenium(III) complexes. This may be due to higher d-orbital energies of the rhenium(III) ion as evidenced from the redox potentials.

The 4d and 5d members of the group 7 and 8 elements, rhenium, ruthenium, and osmium, and less frequently radioactive technetium, continuously draw attention because of versatile redox and photochemical properties of their complexes.[1] They are also important as comparative elements of their 3d members, manganese and iron, which are among the most common biological metal elements. Versatility of the complexes of the four elements come from the fact that they take various oxidation states and yet they are relatively substitution inert in most of the oxidation states. A well recognized difference between the two groups in lower oxidation states is that, while the chemistry of the group 7 elements, technetium and rhenium, is dominated by the complexes with metal–metal bonds, the group 8 elements, ruthenium and osmium, have less tendency to form di- and polynuclear complexes.[1] Although a number of monomeric ruthenium and osmium complexes with various simple common ligands such as ammonia, ethylenediamine, or water are known, most of mononuclear rhenium and technetium complexes of lower oxidation states have been limited to those with a π-acceptor such as CO or phosphine to decrease the electron density on the metals. Recently, it has been recognized that the mononuclear complexes are also stable in rhenium +2 and +3 oxidation states with common nitrogen ligands such as ammonia, ethylenediamines or pyridine derivatives.[2–4] For the trivalent oxidation states, for example, the complexes such as *trans*-$[MCl_2(en)_2]^+$, *trans*-$[MCl_2(NH_3)_4]^+$, and *cis*-$[MCl_2(bpy)_2]^+$ (bpy = 2,3′-bipyridine) are available. Thus, it is interesting to compare the detailed structures, electronic spectra, and redox properties of these rhenium(III) complexes with those of isostructural ruthenium(III), and/or osmium(III) complexes. However, the only set of X-ray structures available for comparison is *cis*-$[ReCl_2(bpy)_2]^+$ and *cis*-$[RuCl_2(bpy)_2]^+$. Redox potentials M(II/III) and M(III/IV) are not always available for a set of complexes, because the Ru complexes tend to take a lower oxidation state as compared with other two metal ions. It is generally observed that osmium complexes have

---

Present Address: Department of Applied Chemistry, Faculty of Engineering, Nagasaki University, Bunkyo-machi, Nagasaki 852-8521

more negative redox potentials as compared with those of analogous ruthenium complexes by ca. 0.4–0.8 V. Limited data seem to suggest that rhenium complexes have even more negative redox potentials, by ca. 0.4–0.8 V as compared with analogous osmium complexes. No meaningful comparison of the electronic spectra has been made among the identical trivalent metal complexes of the three elements. Therefore, further comparison of structural, spectroscopic and redox properties of structurally similar complexes between the rhenium and the two group 8 elements are needed in order to understand the inherent characteristics of these metal ions.

We have been studying the structures, and redox and electronic properties of some dinuclear complexes with the core structures $M_2(\mu\text{-O})(\mu\text{-RCO}_2)_n$ and $M_2(\mu\text{-O})_n$ (n = 1, 2) (M = Fe,[5–7] Ru,[8–23] Os,[24] Re[25–27]) with pyridine and polypyridyl ligands such as tris(2-pyridylmethyl)amine (tpa), 2,2′-bipyridine (bpy), and 1,10-phenanthroline (phen). We have also reported mononuclear rhenium(IV)[28] and -(V) complexes of pyridyl ligands.[29–32] In the course of the study, we have synthesized isostructural complexes $[\mathrm{M^{III}Cl_2(L)}]^+$ (M = Ru, Os, Re; L = tpa and (6-methyl-2-pyridylmethyl)bis(2-pyridylmethyl)amine (Metpa)). These complexes provide a unique opportunity for the comparative studies of the complexes of the three trivalent metal ions with the same ligand set. We report here the syntheses, characterization and electronic and redox properties of the complexes of $[\mathrm{M^{III}Cl_2(L)}]^+$ (M = Ru , L = tpa (**1**), Metpa (**1a**); M = Os, L = tpa (**2**); M = Re, L = tpa (**3**), Metpa (**3a**)) in a comparative way. The present work shows the first example of the set of trivalent metal complexes of the three elements whose X-ray structures have been determined and for which both reduction and oxidation potentials have been clearly observed. During the course of the study, parts of the work have appeared; namely, [**1**]$\mathrm{ClO_4}$[33] and [**3**]$\mathrm{PF_6}$[3] have been reported with the crystal structure of the former. These results are included in our comparative studies.

Experimental

Materials. The ligands tris(2-pyridylmethyl)amine (tpa)[34] and ((6-methyl-2-pyridylmethyl)bis(2-pyridylmethyl)amine (Metpa),[35] and the starting materials $[\mathrm{ReOCl_3(PPh_3)_2}]$ ($\mathrm{PPh_3}$ = $\mathrm{P(C_6H_5)_3}$)[36] and $[\mathrm{RuCl_2(dmso)_4}]$[37] (dmso: dimethyl sulfoxide) were prepared as described in the references. Acetonitrile was dried over calcium hydride and distilled under argon atmosphere. Dichloromethane was dried over diphosphorus pentoxide and distilled under argon atmosphere. Tetrabutylammonium hexafluorophosphate ($\mathrm{TBAPF_6}$) was recrystallized twice from ethanol. All other commercially available reagents were used as purchased.

Preparation of the Complexes. $[\mathrm{Ru^{III}Cl_2(tpa)}]\mathrm{BF_4}$ ([1] $\mathrm{BF_4}$). Method a. The complex was prepared by a method similar to that for $[\mathrm{RuCl_2(tpea)}]\mathrm{ClO_4}$ (tpea = tris(2-pyridylethyl)amine)).[38] $\mathrm{K_2[RuCl_5(H_2O)]}$ (0.37 g, 1.0 mmol) was suspended in 150 mL of ethanol. An ethanolic solution (150 mL) of tpa (0.31 g, 0.1 mmol) was added dropwise to the suspension under reflux. The mixture was refluxed for 24 h, during which time the color changed to reddish brown. Undissolved material was removed by filtration. A small amount of concentrated HCl was added to the filtrate, and the solution was concentrated to ca. 50 mL. On addition of $\mathrm{NH_4BF_4}$ (0.22 g (2 mmol) in a small amount of water) to the solution, brown powder precipitated, this was filtered off, washed with ethanol and diethyl ether, and dried in air. Recrystallization of the precipitate from 2 M HCl gave reddish brown needles. Yield, 0.16 g (29%).

Method b. A methanolic solution (50 mL) of $\mathrm{RuCl_3{\cdot}3H_2O}$ (0.26 g, 1.0 mmol) and tpa (0.29 g, 1.0 mmol) was refluxed for 8.5 h under argon atmosphere and the mixture was cooled to room temperature. After filtration, the methanolic solution of $\mathrm{NH_4BF_4}$ (0.22 g, 2 mmol/5 mL) was added to the filtrate. Yellowish brown microcrystalline powder was filtered off, washed with methanol and diethyl ether successively, and dried in air. Yield 0.47 g (85%). Anal. Calcd for $\mathrm{C_{18}H_{18}N_4BCl_2F_4Ru}$ (FW 549.15): C, 39.37; H, 3.30; N, 10.20; Cl, 12.91%. Found: C, 39.67; H, 3.52; N, 10.35, Cl, 12.83%. IR (KBr) 324, 296 $\mathrm{cm^{-1}}$ (ν(Ru–Cl)). FAB MS m/z 462 ($[\mathrm{RuCl_2(tpa)}]^+$). Hexafluorophosphate and perchlorate salts were obtained by both methods on addition of $\mathrm{NH_4PF_6}$ and $\mathrm{LiClO_4}$, respectively, in place of $\mathrm{NH_4BF_4}$.

$[\mathrm{Ru^{III}Cl_2(Metpa)}]\mathrm{BF_4}$ ([1a]$\mathrm{BF_4}$). This complex can be prepared similarly to the methods a and b for [**1**]$\mathrm{BF_4}$ by using Metpa (0.33 g, 0.1 mmol) instead of tpa. Yield, method a, 0.14 g (25%); method b, 0.45 g (89%). Anal. Calcd for $\mathrm{C_{19}H_{20}N_4BCl_2F_4Ru}$ (FW 563.17): C, 40.52; H, 3.58; N, 9.95%. Found: C, 40.35; H, 3.75; N, 9.79%. IR (KBr) 320, 294 $\mathrm{cm^{-1}}$ (ν(Ru–Cl)).

$[\mathrm{Os^{III}Cl_2(tpa)}]\mathrm{PF_6}$ ([2]$\mathrm{PF_6}$). The ligand tpa (1.14 g, 4.0 mmol) in a small amount of ethanol was added to a solution of $\mathrm{OsO_4}$ (1.0 g, 4.0 mmol) in ethanol (30 mL)–conc. HCl (5 mL). On refluxing the yellow solution for 1 h, yellowish brown precipitate deposited gradually. After the filtration, the precipitate was dissolved in 30 mL of ethyleneglycol. The solution was refluxed for 30 min, during which time the color of the solution changed from yellow to light-green. Ammonium hexafluorophosphate (5.0 g, 30 mmol) was added to the solution, which was then kept in a refrigerator for 1 d. Greenish brown precipitate was filtered off, washed with water and diethyl ether successively, and dried in vacuo. Yield 1.52 g (56%). Anal. Calcd for $\mathrm{C_{18}H_{18}N_4Cl_2F_6POs}$ (FW 696.44): C, 31.04; H, 2.61; N, 8.05%. Found: C, 31.24; H, 2.57; N, 8.22%. Single crystals suitable for X-ray structural determination were obtained by recrystallization of the precipitate from acetonitrile–diethyl ether. The crystals contain one molecule of diethyl ether per complex. FAB MS m/z 552 ($[\mathrm{Os^{III}Cl_2\ (tpa)}]^+$). IR (KBr): 320, 298 $\mathrm{cm^{-1}}$ (ν(Os–Cl)).

$[\mathrm{Re^{III}Cl_2(tpa)}]\mathrm{BF_4}$ ([3]$\mathrm{BF_4}$). A suspension of $[\mathrm{ReOCl_3(PPh_3)_2}]$ (0.3 g, 0.4 mmol) and tpa (0.11 g, 0.4 mmol) in 15 mL of ethanol was refluxed for 20 min. The yellow suspension changed to orange and then to a clear red solution. After cooling, $\mathrm{NH_4BF_4}$ (0.10 g, 0.95 mmol) in 5 mL of water was added to the solution. Red microcrystalline precipitate was filtered off, washed with diethyl ether and dried in vacuo. Recrystallization of the product from acetonitrile-diethyl ether gave red crystals, which were suitable for X-ray structural determination. Yield 0.21 g (80%). Anal. Calcd for $\mathrm{C_{18}H_{18}N_4BCl_2F_4Re}$ (FW 634.28): C, 34.09; H, 2.86; N, 8.83%. Found: C, 34.17; H, 2.96; N, 8.94%. FAB MS m/z 547 ($[\mathrm{ReCl_2\ (tpa)}]^+$). IR (KBr) 318, 294 $\mathrm{cm^{-1}}$ (ν(Re–Cl)).

$[\mathrm{Re^{III}Cl_2(Metpa)}]\mathrm{BF_4}$ ([3a]$\mathrm{BF_4}$). The complex was prepared similarly to that of [**3**]$\mathrm{BF_4}$ by using Metpa instead of tpa. Recrystallization from acetonitrile–diethyl ether gave red crystals, which were suitable for X-ray structural determination. Yield 0.19 g (75%). Anal. Calcd for $\mathrm{C_{19}H_{20}N_4BCl_2F_4Re}$ (FW 648.31): C, 35.20; H, 3.11; N, 8.64%. Found: C, 35.53; H, 3.50; N, 8.31%. FAB MS m/z 561 ($[\mathrm{ReCl_2(Metpa)}]^+$). IR (KBr) 312, 288 $\mathrm{cm^{-1}}$ (ν (Re–Cl)).

$[\mathrm{Ru^{II}Cl(dmso)(tpa)}]\mathrm{PF_6}$ ([4]$\mathrm{PF_6}$). This complex has been independently reported recently.[39] A mixture of $[\mathrm{RuCl_2(dmso)_4}]$ (0.3 g, 0.6 mmol) and tpa (0.17 g, 0.6 mmol) in 20 mL of ethanol was refluxed for 4 h under argon atmosphere. Ammonium hexafluorophosphate (0.15 g, 0.9 mmol) in ethanol (5 mL) was added to the solution. Yellow microcrystalline precipitate was filtered off, washed with ethanol and air dried. Yield 0.35 g (90%). Anal. Calcd for $C_{20}H_{24}N_4OSClF_6PRu$ (FW 649.99): C, 36.96; H, 3.72; N, 8.62; S, 4.93; Cl, 5.45%. Found: C, 36.99; H, 3.83; N, 8.52; S, 4.92; Cl, 5.46%. FAB MS *m/z* 505 ([RuCl (dmso) (tpa)]$^+$). UV-vis (CH_3CN) 362 (ε 10700 mol dm^3 cm^{-1}), 316 (6700), 249 nm (16600).

[Ru^{II}Cl(dmso)(Metpa)]PF$_6$ ([4a]PF$_6$). The complex was prepared similarly to that of [**4**][PF$_6$] by using Metpa instead of tpa. Anal. Calcd for $C_{21}H_{26}N_4OSPClF_6Ru$ (FW 664.02): C, 39.67; H, 3.52; N, 10.35%. Found: C, 39.37; H, 3.31; N, 10.20%. UV-vis (CH_3CN) 360 (ε 9770 mol dm^3 cm^{-1}), 316 (6150), 248 nm (16400). ^{1}H NMR spectra of these complexes in CD_3CN gave ligand signals in the normal diamagnetic region and show no sign of the existence of more than two geometrical or linkage isomers.

X-ray Structural Determinations. X-ray data of [**1a**]BF$_4$, [**3**]BF$_4$, and [**3a**]BF$_4$ were collected with graphite-monochromated Mo *Kα* radiation on a MacScience MXC 18 diffractometer at 20 °C. Unit cell parameters were obtained by least-squares refinement of 26 reflections ($30 < 2\theta < 35°$). The intensities of three standard reflections, monitered every 100 reflections, showed no decay. X-ray data of [**2**]PF$_6$·$C_2H_5OC_2H_5$ was collected with graphite-monochromated Mo *Kα* radiation on a Rigaku AFC-5R diffractometer at 20 °C. Unit cell parameters were obtained by least-squares refinement of 25 reflections ($25 < 2\theta < 30°$). The intensities of three standard reflections, monitered every 150 reflections, showed no decay. Further crystallographic data are summarized in Table 1. The structures of [**1a**]BF$_4$, [**2**]PF$_6$·$C_2H_5OC_2H_5$, [**3**]BF$_4$, and [**3a**]BF$_4$ were solved by the heavy-atom method (DIRDIF)[40] and expanded using Fourier techniques. The 6-methyl-2-pyridyl group in [**1a**]BF$_4$ was disordered on the two positions. The occupancy factor of 0.5 was assigned to each of the methyl carbon atoms C(1) and C(2). For [**2**]PF$_6$·$C_2H_5OC_2H_5$, H atoms were included at calculated positions with fixed displacement parameters (1.2 times the displacement parameters of the hosy atom). All calculations were performed using CRYSTAN[41] for [**1a**]BF$_4$, [**3**]BF$_4$ and [**3a**]BF$_4$ and TEXSAN[42] for [**2**]PF$_6$·$C_2H_5OC_2H_5$. Selected bond distances and angles are summarized in Table 2.

X-ray crystallographic files in CIF format for [**1a**]BF$_4$, [**2**]PF$_6$·$C_2H_5OC_2H_5$, [**3**]BF$_4$, and [**3a**]BF$_4$ have been deposited as document No. 74056 at the office of the Editor of Bull. Chem. Soc. Jpn. and also deposited at the CCDC, 12 Union Road, Cambridge CB21EZ, UK and copies can be obtained on request, free of charge, by quoting the publication citation and the deposition numbers 168203–168202.

Electrochemical Measurements. Cyclic voltammetry was performed with a Hokuto HA-501 potentiostat and a Hokuto HB-105 function generator equipped with a Graphtec WX2400 X-Y recorder. The working and the counter electrodes were a glassy-carbon disk and a platinum wire, respectively. Cyclic voltammograms were recorded at a scan rate of 50 mV/s. The sample solutions (ca. 1.0 mM) in 0.1 M TBAP$_6$–acetonitrile were deoxygenated with a stream of nitrogen gas. The reference electrode was Ag/AgCl and the half-wave potentials of Fc$^+$/Fc ($E_{1/2}$ (Fc$^{+/0}$) vs Ag/AgCl was 0.435 V and 0.43 V in CH_3CN and CH_2Cl_2, respectively.

Other Measurements. Electronic spectra were recorded on a Hitachi 3000U spectrophotometer at 20 °C. IR spectra were recorded on a Hitachi 270-50 infrared spectrophotometer. ^{1}H NMR spectra were measured on a JEOL-EX 270 (270 MHz) spectrometer.

Results and Discussion

Preparation of the Complexes. We have successfully prepared a series of the complexes [MCl$_2$(L)]$^+$ (L = tpa, Me-

Table 1. Crystallographic Data for [**1a**]BF$_4$, [**2**]PF$_6$·$C_2H_5OC_2H_5$, [**3**]BF$_4$ and [**3a**]BF$_4$

	[**1a**]BF$_4$	[**2**]PF$_6$·$C_2H_5OC_2H_5$	[**3**]BF$_4$	[**3a**]BF$_4$
Formula	$C_{19}H_{20}N_4BCl_2F_4Ru$	$C_{22}H_{28}N_4Cl_2F_6OsP$	$C_{18}H_{18}N_4BCl_2F_4Re$	$C_{19}H_{20}N_4BCl_2F_4Re$
Fw	563.2	770.6	634.3	648.3
Space group	$P2_1/a$ (no.14)	$P2_1/a$ (no.14)	$P2_12_12_1$ (no.19)	$P2_1/a$ (no.14)
T/ °C	20	20	20	20
a/ Å	14.665(7)	15.680(2)	15.327(3)	15.273(5)
b/ Å	15.106(8)	12.092(3)	15.949(3)	12.721(4)
c/ Å	10.619(4)	16.149(2)	8.723(2)	12.574(4)
β/ deg	106.51(4)	111.994(9)		91.68(3)
V/ Å^3	2255(2)	2839.0(7)	2132.4(8)	2442(1)
Z	4	4	4	4
D_{calcd}/g cm^{-3}	1.68	1.80	2.12	1.76
Cryst size/mm	0.40 × 0.20 × 0.18	0.56 × 0.14 × 0.12	0.50 × 0.20 × 0.10	0.45 × 0.12 × 0.05
Scan range/deg	$1.71 + 0.35\tan\theta$	$1.42 + 0.30\tan\theta$	$1.11 + 0.35\tan\theta$	$1.52 + 0.35\tan\theta$
Scan mode	ω-2θ	ω-2θ	ω-2θ	ω-2θ
Scan speed	6°	4°	6°	8°
$2\theta_{max}$/deg	50	50	60	50
μ (Mo $K\alpha$)/ cm^{-1}	7.23	47.95	58.17	53.07
Abs corr	none	psi-Scans	numerical	psi-Scans
No. of unique reflns	4611	5265	3517	4942
No. of obsd reflns	3179, $I > 1.5\sigma(I)$	3715, $I > 2\sigma(I)$	2927, $I > 2\sigma(I)$	2986, $I > 1.5\sigma(I)$
$R^{a)}$ (%)	4.9	3.0	4.2	4.4
$R_w{}^{a)}$ (%)	5.2	4.1	4.4	5.8

a) $R = \Sigma||F_0| - |F_c||/\Sigma|F_0|$. $R_w = [\Sigma_w (|F_0| - |F_c|)^2/\Sigma_w|F_0|^2]^{1/2}$.

Table 2. Selected Bond Lengths (Å) and Bond Angles (°) for for [**1a**]BF_4, [**2**]$PF_6 \cdot C_2H_5OC_2H_5$, [**3**]BF_4 and [**3a**]BF_4 and [$RuCl_2$(tpa)] ClO_4 ([**1**]ClO_4)

	Bond Lengths (Å)				
	[**1a**]BF_4	[**2**]$PF_4 \cdot C_2H_5OC_2H_5$	[**3**]BF_4	[**3a**]BF_4	[**1**]ClO_4
M–Cl(1)	2.377(3)	2.366(2)	2.353(4)	2.371(4)	2.330(2)
M–Cl(2)	2.362(2)	2.367(2)	2.389(4)	2.386(4)	2.357(2)
M–N(1)	2.067(5)	2.071(5)	2.130(9)	2.130(11)	2.068(5)
M–N(11)	2.086(6)	2.077(5)	2.099(10)	2.114(12)	2.087(5)
M–N(21)	2.095(6)	2.066(6)	2.094(8)	2.153(12)	2.073(5)
M–N(31)	2.114(6)	2.070(5)	2.105(9)	2.161(11)	2.074(5)

	Bond Angles (°)				
	[**1a**]BF_4	[**2**]$PF_6 \cdot C_2H_5OC_2H_5$	[**3**]BF_4	[**3a**]BF_4	[**1**]ClO_4
Cl(1)–M–Cl(2)	91.4(1)	92.22(6)	92.5(2)	92.5(2)	91.21(7)
Cl(1)–M–N(1)	175.0(2)	175.5(2)	174.8(3)	171.0(4)	175.9(2)
Cl(1)–M–N(11)	93.5(2)	94.3(1)	94.4(3)	93.9(4)	
Cl(1)–M–N(21)	99.7(2)	97.0(2)	101.1(3)	92.4(4)	
Cl(1)–M–N(31)	98.4(2)	99.5(2)	99.3(3)	108.6(4)	
Cl(2)–M–N(1)	93.3(2)	91.6(2)	92.7(3)	92.1(4)	
Cl(2)–M–N(11)	174.5(2)	172.3(2)	172.3(3)	173.5(4)	175.0(2)
Cl(2)–M–N(21)	90.0(2)	88.4(2)	91.2(3)	91.4(4)	
Cl(2)–M–N(31)	88.9(2)	90.2(2)	89.4(3)	88.6(4)	
N(1)–M–N(11)	82.8(3)	82.1(2)	80.5(4)	81.6(5)	82.8(2)
N(1)–M–N(21)	82.0(2)	80.8(2)	79.5(4)	79.8(5)	81.8(2)
N(1)–M–N(31)	80.0(3)	82.8(2)	80.0(4)	79.2(5)	81.3(2)
N(11)–M–N(21)	86.8(3)	95.0(2)	85.0(4)	89.3(5)	
N(11)–M–N(31)	92.7(3)	84.6(2)	92.0(4)	88.5(5)	
N(21)–M–N(31)	161.9(3)	163.5(2)	159.6(4)	159.0(5)	163.1(2)

tpa) for the three different trivalent metal ions: Ru(III), Os(III), and Re(III). Preparation methods adopted here are quite different for each of the three metal ions because of their different reactivity and the availability of the starting materials.

For ruthenium, an analogous complex, [$RuCl_2$(tpea)] ClO_4 (tpea = tris(2-pyridylethyl)amine) has been prepared previously from $K_2[Ru^{III}Cl_5(H_2O)]$ by Che and co-workers.[38] Kojima also has prepared [$Ru^{III}Cl_2$(tpa)]ClO_4 ([**1**]ClO_4) by using the same starting material.[33] We have obtained [**1**]BF_4 and [**1a**]BF_4 by the reaction of tpa with [$RuCl_3 \cdot 3H_2O$] as well as with $K_2[Ru^{III}Cl_5(H_2O)]$. The former gave [**1**]BF_4 in much higher yield. When the Ru(II) complex, [$RuCl_2(dmso)_4$],[37] was used as a starting material, the reaction with tpa or Metpa gave monochlororuthenium(II) complexes of [RuCl(dmso)(L)]PF_6 (L = tpa, [**4**]PF_6;[39] Metpa, [**4a**]PF_6). The reaction of [$Ru_3(CO)_{12}$] with tpa afforded a carbonyl containing tpa complex [$Ru(CH_3COO)(CO)$(tpa)]$^+$.[43,44]

In the case of the preparation of [$OsCl_2$(tpa)]$^+$ [**2**]$^+$, we have used two different starting materials, $(NH_4)_2[Os^{IV}Cl_6]$ and OsO_4. The reaction of the former with tpa in ethyleneglycol gave a salt of [$OsCl_2$(tpa)]$_2$[$OsCl_6$][45] which was sparingly soluble in water, dichloromethane and acetonitrile, and an attempt to convert it into a salt of other anions was not made. When OsO_4 was employed as a starting material, complex [**2**]PF_6 was obtained through an unidentified intermediate. It is interesting to note that five electron reduction occurred during the preparation of the Os(III) complex without using any reducing reagent. The complex [**2**]PF_6 was soluble in acetonitrile, acetone, dichloromethane, and dimethylformamide.

The chemistry of Re(III) is significantly different from those of the trivalent states of the other two elements in the sense that the low valent Re(III) has a tendency to form complexes with the Re–Re multiple bonds.[1] It seems that this does not mean that mononuclear rhenium complexes are unstable but less attention has been paid to them because of much interest to the Re-Re bonded complexes. It has now been recognized, however, that some stable mononuclear Re(III) complexes can be prepared with common nitrogen ligands. Harman and co-workers reported *trans*-dichlororhenium(III) complexes, *trans*-[$ReCl_2(en)_2$]$^+$, *trans*-[$ReCl_2(NH_3)_4$]$^+$ and *trans*-[$ReCl_2(ampy)_2$]$^+$ (en = ethylenediamine; ampy = 2-(aminomethyl)pyridine), which were prepared from *trans*-[$Re(O)_2(en)_2$]$^+$, *trans*-[$Re(O)_2(NH_3)_4$]$^+$ and *trans*-[$Re(O)_2(ampy)_2$]$^+$, respectively, in HCl solution.[2] *cis*-Dichlororhenium(III) complexes, [**3**]BF_4 and [**3a**]BF_4 were prepared by the reaction of [$Re^{V}OCl_3(PPh_3)_2$] with tpa and Metpa, respectively, in refluxing ethanol. The salts of BF_4^-, PF_6^- and ClO_4^- have also been obtained by adding NH_4BF_4, NH_4PF_6, and $NaClO_4$, respectively, to the reaction mixture. Previously, we have found that a Re(V) complex of [$ReO(OCH_3)$(tpa)]$(PF_6)_2$ formed when the reaction was carried out in CH_3OH at room temperature for several days.[29] In the mixed solvent of ethanol–H_2O (1 : 1 v/v), however, the reflux of the same reaction mixture gave dimeric species [$Re^{III}Re^{IV}(\mu\text{-}O)_2(L)_2$]$^{3+}$ (L = tpa, Metpa).[27] A disproportionation mechanism has been proposed, since the salt of ReO_4^- has been isolated. The monooxo bridged Re(III) dimer,

$[\mathrm{Re^{III}}_2\ (\mu\text{-O})\mathrm{Cl_2(tpa)_2}]^{2+}$, has also been obtained under slightly different reaction conditions.[46] In the case of the preparation of the present monomeric Re(III) complexes, disproportionation mechanism to produce Re(III) is unlikely, since the yields of [**3**]$\mathrm{BF_4}$ and [**3a**]$\mathrm{BF_4}$ are rather high. Instead, intra- or intermolecular oxygen abstraction by $\mathrm{PPh_3}$ leading Re(V) to Re(III) is more likely to take place. In fact, the reaction of $[\mathrm{Re^{V}OCl_2}(\kappa^3\text{-tpa})]$[29] with $\mathrm{PPh_3}$ gave the Re(III) complex $[\mathrm{ReCl_2(tpa)}]^{+}$. The reactions were carried out in $\mathrm{CH_2Cl_2}$, $\mathrm{CH_3CN}$, or $\mathrm{CH_3COCH_3}$ in air or under argon atmosphere with the reaction times of a few hours at room temperature. Thus, we have demonstrated that the reaction of $[\mathrm{Re^{V}OCl_3(PPh_3)_2}]$ with the tpa gave monomeric Re(III) and Re(V) complexes, and dimeric mono-μ-oxo Re(III)Re(III), and di-μ-oxo Re(III)Re(IV) (and also Re(IV)Re(IV)) complexes, under different reaction conditions. On the other hand, the reaction of $[\mathrm{ReOCl_3((CH_3)_2S)(OPPh_3)}]$ with tpa did not give any Re(III) complex. It is interesting to note that a similar reaction of $[\mathrm{ReOCl_3\ (PPh_3)_2}]$ with a pentadentate ligand 2,2′:6′,2″:6″,2‴:6‴,2⁗-quinquepyridine (qpy) and a hexadenate ligand *N*,*N*,*N′*,*N′*-tetrakis(2-pyridylmethyl)ethylenediamine (tpen) afforded seven coordinate complexes, *trans*-$[\mathrm{Re^{III}Cl_2(qpy)}]\mathrm{ClO_4}$[47] and $[\mathrm{ReO\ (tpen)}]^{n+}$ ($n = 2$, 3),[28] respectively. Recently, the tpa complex [**3**]$\mathrm{PF_6}$ has been prepared independently by Harman and co-workers.[3] They used $[\mathrm{Re^{III}(benzil)(PPh_3)Cl_3}]$ as a starting material and obtained the product in 65% yield by refluxing it with tpa for 72 h in benzene. In our method, the complex can be easily synthesized at higher yield by refluxing only for 20 min.

General Features of the Structures. Figures 1, 2, 3 and 4 display the crystal structures of the complex cations in $[\mathrm{RuCl_2(Metpa)}]\mathrm{BF_4}$ ([**1a**]$\mathrm{BF_4}$), $[\mathrm{OsCl_2(tpa)}]\mathrm{PF_6}$ ([**2**]$\mathrm{PF_6}$), $[\mathrm{ReCl_2(tpa)}]\mathrm{BF_4}$ ([**3**]$\mathrm{BF_4}$), and $[\mathrm{ReCl_2(Metpa)}]\mathrm{BF_4}$ ([**3a**]$\mathrm{BF_4}$), respectively. Selected bond distances and angles of these complexes are summarized in Table 2 together with those of $[\mathrm{RuCl_2(tpa)}](\mathrm{ClO_4})$ ([**1**]$\mathrm{ClO_4}$).[33] All these complex cations are structurally very similar to each other. Each metal ion takes a distorted octahedral coordination environment with four nitrogens of the tetradentate ligand tpa or Metpa and two chloride ions. The 6-methyl-2-pyridyl group in [**1a**]$\mathrm{BF_4}$ is disordered on the two positions (corresponding to N(21) and N(31)) *cis* to both the chloride ligands. Accordingly Cl(1) atom may be in a small disorder to avoid steric hindrance of methyl group on the pyridyl ring, as indicated by its large temperature factor. On

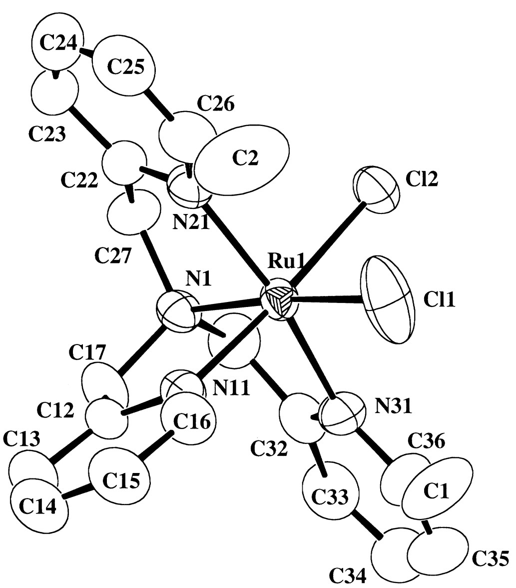

Fig. 1. Molecular structure of complex cation of $[\mathrm{RuCl_2(Metpa)}]\mathrm{BF_4}$ ([**1a**]$\mathrm{BF_4}$) with the atomic numbering scheme showing 50% probability thermal ellipsoids.

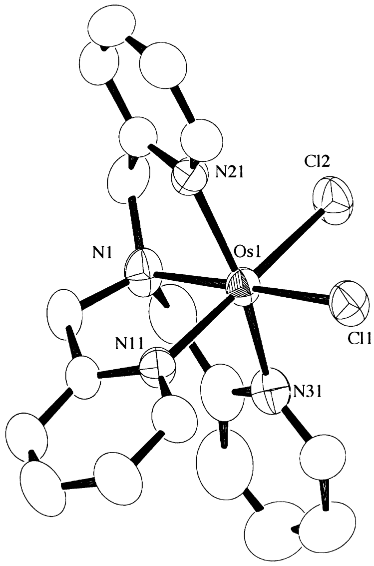

Fig. 2. Molecular structure of complex cation of $[\mathrm{OsCl_2(tpa)}]\mathrm{PF_6}$ ([**2**]$\mathrm{PF_6}$) with the atomic numbering scheme showing 50% probability thermal ellipsoids.

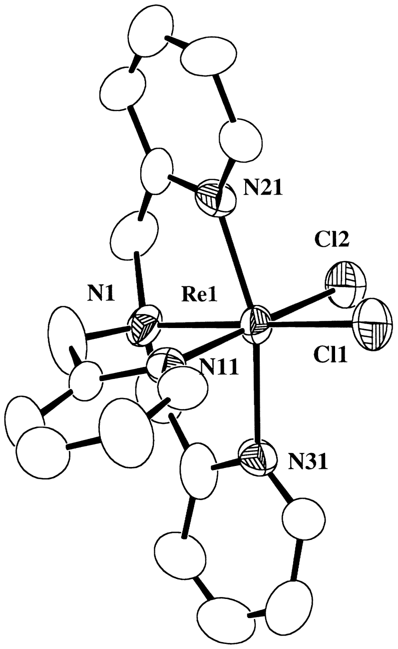

Fig. 3. Molecular structure of complex cation of $[\mathrm{ReCl_2(tpa)}]\mathrm{BF_4}$ ([**3**]$\mathrm{BF_4}$) with the atomic numbering scheme showing 50% probability thermal ellipsoids.

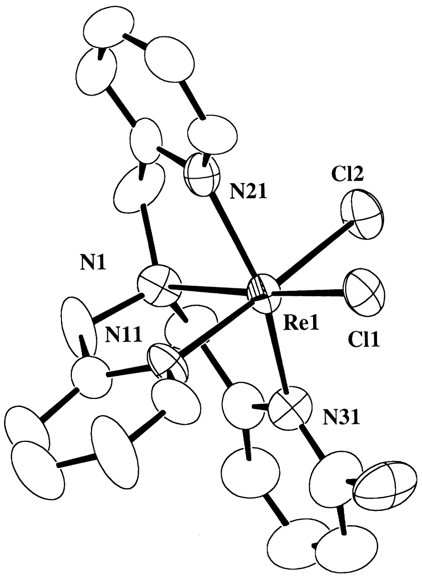

Fig. 4. Molecular structure of complex cation of $[ReCl_2(Metpa)]BF_4$ ([**3a**]BF_4) with the atomic numbering scheme showing 50% probability thermal ellipsoids.

the other hand, the substituent methyl group in the complex [**3a**]BF_4 is not disordered. The two chloride ions in each of the five complexes are non-equivalent, one is at the position *trans* to the tertiary nitrogen N(1) and the other is *cis* to it. The difference between M–Cl(1) and M–Cl(2) distances is larger for [**3**]BF_4 and [**1**]ClO_4[33] than that for the other three complexes. It is difficult to explain this observation fully at this stage. However, it is noteworthy here that the [**3**]BF_4 and [**1**]ClO_4 crystallized in a chiral space group $P2_12_12_1$, indicating that the spontaneous resolution was occurred for these complexes. On the other hand, in the complexes of [**1a**]BF_4, [**2**]PF_6, and [**3a**]BF_4 which crystallized in an achiral space group $P2_{1/a}$, two M–Cl distances are similar to each other. The difference of the crystal packing might affect the M–Cl distances by some extent. With regard to the difference of the four M–N bond lengths, there is no systematic trend among the five complexes. Average bond lengths of M–N(pyridyl) in [**3**]BF_4 (2.099 Å) and [**3a**]BF_4 (2.142 Å) are slightly longer than the corresponding value in *cis*-$[ReCl_2(bpy)_2]$ PF_6 (2.095 Å).[3]

Structural Dependence on the Metal Ions and Ligand Methyl Substituents. Structural parameters of the tpa complexes of Ru and Os ([**1**]ClO_4, [**2**]PF_6) are very similar to each other, and the difference in corresponding bond lengths is less than 0.01 Å except for the M–Cl(1) bond which is *trans* to the tertially nitrogen. The bond lengths in the Re tpa complex [**3**]BF_4 are apparently longer than the corresponding ones of the other two tpa complexes, again except for the M–Cl(1) bond. Thus the general trend of the bond-lengths is in the order Re–L > Os–L ~ Ru–L. Although the precise ionic radii of all the three trivalent metal ions are not available, the order is as expected from the general tendency of ionic radius; (i) the ionic radii of second and third raw metal ions of the same group are similar, and (ii) the ionic radii in the same transition series decrease with the increasing atomic number if d-electron configuration is not significantly influential. Both Re(III) and Os(III) in the present case take low spin states with no electron in dσ orbilals.

Careful inspection of the data for tpa complexes in Table 2 reveals a few characteristic features. It is seen that Re–N(pyridyl) distances (average: 2.104 Å) in [**3**]BF_4 are longer as compared with those of the d^5 Os and Ru complexes and such differences are explained by the lesser extent of π-back donation of the d^4 Re complexes. Such π-back donation is typically seen in the complexes, $[Ru^{II}Cl_2(bpy)_2]\cdot 3.5H_2O$ and $[Ru^{III}Cl_2(bpy)_2]\ Cl\cdot 2H_2O$, where the Ru^{II} (d^6)–N distances are shorter in spite of the bigger ionic radius ($\Delta d = d\,(Ru^{III}\text{–}N) - d\,(Ru^{II}\text{–}N) = 0.022$ Å).[48] Although the difference is small, further detailed comparison of the data of [**1**]ClO_4 and [**2**]PF_6 shows that while the M–Cl and M–N(amine) bond lengths are slightly longer for the osmium complex, the M–N(pyridyl) ones are slightly longer for the ruthenium complex. Namely, the Ru–N(pyridyl) bonds (average: 2.078 Å) in [**1**]ClO_4 are longer than Os–N bonds (average: 2.071 Å) in [**2**]PF_6. It is possible that the back-donation to the pyridyl π^* orbitals is more favorable for the Os(III) complex where dπ orbital energy is higher and closer to the ligand π^* orbitals.

The longer M–N(pyridyl) distance in the rhenium complex [**3**]BF_4 appears to cause further influence to its coordination environment. The Re–N(amine) bond in [**3**]BF_4 is significantly longer than those of [**1**]ClO_4 and [**2**]PF_6 by ca. 0.06 Å. With increasing bond-lengths of the three Re–N(pyridyl) bonds, the Re–N(amine) bond must take a longer distance in order to release the steric strain of the ligand configuration. Such a steric consideration is supported by a more distorted structure of the rhenium complexes, as typically seen in the N(21)–Re–N(31) angle (159.6(4)°) which is ca. 4° smaller than that of Ru and Os complexes. The weakening of the Re–N(amine) bond would then cause shortening of the *trans* Re–Cl(1) bond.

The major stereochemical change caused by the introduction of a methyl substituent on one of the pyridyl groups is explained by the steric repulsion between the methyl group and the neighboring coordinated chloride. The methyl group is disordered on the two pyridyl rings in [**1a**]BF_4, and is fixed on the N(31) pyridyl ring in [**3a**]BF_4. For [**1a**]ClO_4, the Ru–N(methylpyridyl) and the Ru–Cl(1) bonds which oriented to the direction of methyl substituent, are significantly longer than the corresponding bonds in the tpa complex, [**1**]BF_4. In [**3a**]BF_4, additional stereochemical change is observed, namely the Cl(1) ligand shifts towards one (N(21)) of the two pyridyl groups which has no methyl substituent as verified by the angles, Cl(1)–Re–N(31) (108.6(4)°), Cl(1)–Re–N(21) (92.4(4)°) and Cl(1)–Re–N(1) (171.0(4)°). This may cause the lengthening of the Re–N(21) bond. Consequently, the coordination geometry of [**3a**]BF_4 is highly distorted from regular octahedron. Structural disorder in [**1a**]BF_4 preclude one from observing such a significant distortion.

To summarize the structural comparison, the somewhat larger ionic radius of Re(III) causes notable differences in the extent of distortion of the coordination geometries, especially the consequence of steric repulsion involving the methyl substituent.

Electrochemistry of the Complexes. Redox potentials of the complexes are summarized in Table 3. As a typical example, cyclic voltammograms of [**3**]BF_4 in various solvents are

Table 3. Electrochemical Data of $[MCl_2(L)]^{n+}$ (M = Ru, Os, Re; L = tpa, Metpa)[a)]

Complex		$E_{p,c}$ (V vs Fc^+/Fc)	$E_{1/2}$[b)] (V vs Fc^+/Fc)	$E_{1/2}$[b)] (V vs Fc^+/Fc)	Solvent	Ref.
		(I) / (II)	(II) / (III)	(III) / (IV)		
$[RuCl_2(tpa)]^{n+}$	(**1**)		−0.24	1.39	d	29
$[RuCl_2(Metpa)]^{n+}$	(**1a**)		−0.23	1.39	d	this work
$[OsCl_2(tpa)]^{n+}$	(**2**)		−0.81	0.79	d	this work
$[ReCl_2(tpa)]^{n+}$	(**3**)	−2.27[d)]/	−1.30[d)]/−1.35[e)]	0.25[c),d)]/0.36[e)]	d/e	this work
$[ReCl_2(Metpa)]^{n+}$	(**3a**)	−2.37[d)]/	−1.32[d)]/−1.35[e)]	0.25[d)]/0.31[e)]	d/e	this work

a) tpa = tris(2-pyridylmethyl) amine, Metpa = (6-methyl-2-pyridylmethyl)bis(2-pyridylmethyl)amine. b) $E_{1/2} = (E_{pa} + E_{pc})/2$, where E_{pa} and E_{pc} are anodic and cathodic peak potentials, respectively. c) Irreversible. d) CH_3CN. e) CH_2Cl_2.

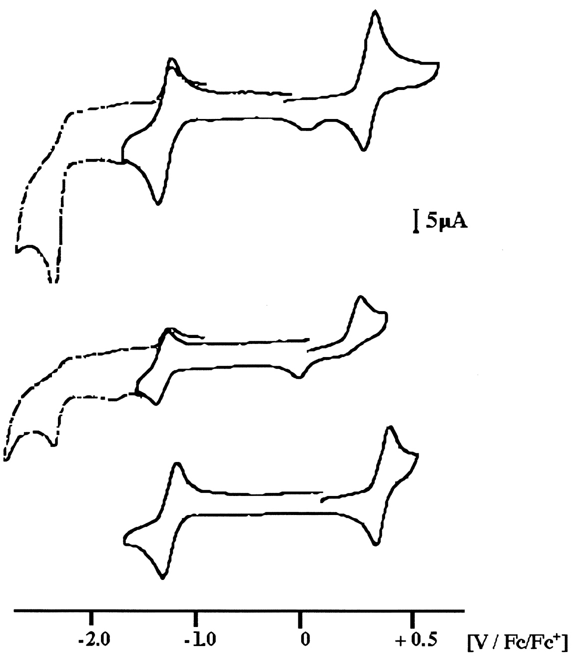

Fig. 5. Cyclic voltammogram of $[ReCl_2(tpa)]BF_4$ ($[\mathbf{3}]BF_4$) in CH_3CN (above), DMF (middle), and CH_2Cl_2 (bottom) solution of $TBAPF_6$ (0.1 M) at a glassy-carbon electrode with a scan rate of 50 m V/s.

shown in Fig. 5. Complexes $[\mathbf{1}]ClO_4$, $[\mathbf{1a}]BF_4$ and $[\mathbf{2}]PF_6$ display two reversible waves; one in the positive potential region (vs Fc/Fc^+) (1.39, 1.39, and 0.79 V, respectively) and the other in the negative region (−0.24, −0.23, and −0.81 V, respectively). These processes are assigned to the M(III/IV) and M(II/III) couples, as shown in Eqs. 1 and 2:

$$[Ru^{II}Cl_2(L)] \rightleftarrows [Ru^{III}Cl_2(L)]^+ \rightleftarrows [Ru^{IV}Cl_2(L)]^{2+} \quad (L = \text{tpa, Metpa}), \qquad (1)$$

$$[Os^{II}Cl_2(tpa)] \rightleftarrows [Os^{III}Cl_2(tpa)]^+ \rightleftarrows [Os^{IV}Cl_2(tpa)]^{2+}. \qquad (2)$$

No further wave was observed in the range up to −2.0 V. Only one wave was observed previously for some related Ru(III) and Os(III) complexes. The ruthenium(III) complexes, *cis*-$[RuCl_2(bpy)_2]^+$, *cis*-$[RuCl_2(NH_3)_4]^+$ and *cis*-$[RuCl_2(en)_2]^+$, show Ru(II/III) processes at 0.56, −0.082, and −0.09 V vs NHE (0.07, −0.57, and −0.58 V (vs Fc/Fc^+)), respectively, in H_2O,[49,50] no oxidation wave being observed. On the contrary, osmium(III) complex *cis*-$[OsCl_2(NH_3)_4]^+$ displays only Os(III/IV) process at +0.82 V vs NHE (+0.33 V vs Fc/Fc^+) in H_2O.[51] Observation of the two redox waves in the present complexes is due mainly to the high solubility toward organic solvents, which makes measurements over a wide potential range region possible.

The rhenium complexes $[\mathbf{3}]BF_4$ and $[\mathbf{3a}]BF_4$ in CH_3CN display three redox processes, assigned as Eq. 3. These processes are reversible except for the Re(III/IV) process of $[\mathbf{3}]BF_4$ and Re(I/II) ones of $[\mathbf{3}]BF_4$, and $[\mathbf{3a}]BF_4$.

$$[Re^{I}Cl_2(L)]^- \rightleftarrows [Re^{II}Cl_2(L)] \rightleftarrows [Re^{III}Cl_2(L)]^+ \rightleftarrows [Re^{IV}Cl_2(L)]^{2+} \qquad (3)$$

The three redox waves were also observed in other rhenium(III) complexes, *trans*-$[ReCl_2(ampy)_2]^+$ (−2.0, −1.15, and +0.53 V vs NHE) and *cis*-$[ReCl_2(bpy)_2]^+$ (−1.01, −0.17, and +1.06 V vs NHE), in dimethylacetamide.[2,3] The redox potentials of $[\mathbf{3}]BF_4$ (converted values vs NHE, −2.00, −1.08, and +0.50 V, respectively) are close to those of *trans*-$[ReCl_2(ampy)_2]^+$, and significantly more negative than the corresponding values of *cis*-$[ReCl_2(bpy)_2]^+$, indicating the importance of the π-back donation to the chelated bpy ligands.

While the Re(III/IV) process of Metpa complex $[\mathbf{3a}]BF_4$ is reversible in CH_3CN, that of tpa complex $[\mathbf{3}]BF_4$ is irreversible in the way that the small reduction wave at E_{pc} = +0.01 V was observed at the expense of the original reduction wave. In a stronger coordinating solvent DMF, the process became irreversible and a new cathodic wave around 0 V became larger and the original reduction wave corresponding to a cathodic process as seen in CH_3CN disappeared. The process remains reversible, however, in non-coordinating solvent CH_2Cl_2. These observations may be ascribed to the dissociation of Cl^- from the coordination sphere by the attack of the solvent molecule at the Re(IV) oxidation state. Helberg and co-workers observed the splitting of the reduction wave in the Re(II/III) process of $[Re(terpy)_2]^{n+}$ in acetone in the presence of Cl^-, CN^-, and ^{t}BuNC, and suggested the participation of a solvent attached seven coordinated species.[3] In the present case, formation of a seven coordinated complex is unlikely, since no seven coordinated non-oxo rhenium(IV) species is known so far. Good reversibility of the Re(III/IV) process of $[\mathbf{3a}]BF_4$ is explained by considering that the steric bulkiness of the methyl substituent makes the solvolysis less favorable. Reversibility of the Ru(III/IV) and Os(III/IV) processes of $[\mathbf{1}]BF_4$ and $[\mathbf{2}]PF_6$, respectively, indicates lesser lability of Ru(IV) and Os(IV). The methyl substituent does not give significant effect on the redox potentials as indicated by the comparative data of the

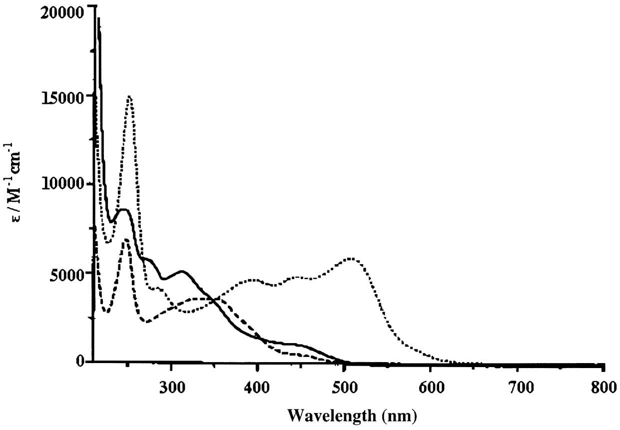

Fig. 6. Absorption spectra of [RuCl$_2$(Metpa)]BF$_4$ ([**1a**] BF$_4$) (solid line), [OsCl$_2$(tpa)]PF$_6$ ([**2**]PF$_6$) (dashed line) and [ReCl$_2$(tpa)] BF$_4$ ([**3**]BF$_4$) (dotted line) in CH$_3$CN.

pair of complexes [**1**]BF$_4$ and [**1a**]BF$_4$, and [**3**]BF$_4$ and [**3a**]BF$_4$.

The complexes of *cis*-[RuCl$_2$(bpy)], *trans*-[OsCl$_2$(NH$_3$)$_4$]$^+$ and *trans*-[OsCl$_2$(en)$_2$]$^+$ did not show the Ru(III/IV) and the Os(II/III) couples, respectively. However, since all the present complexes show redox processes corresponding to M(II/III) and M(III/IV), it is possible to discuss the general trend of the redox potentials of the isostructural complexes of the three metal ions. The corresponding potentials are in the order Ru < Os < Re, with the differences in the potentials of 0.5–0.7 V. It is interesting to note that the difference between the two potentials, M(II/III) and M(III/IV), is similar among the three tpa complexes, [**1**]BF$_4$, [**2**]PF$_6$, and [**3**]BF$_4$ (ΔE = 1.63, 1.60, and 1.71 V, respectively). Since these values correspond to the thermodynamic stability of trivalent oxidation states (= [M$^{\mathrm{II}}$] [M$^{\mathrm{IV}}$] / [M$^{\mathrm{III}}$]^2), the similarity suggests that the number of d-electrons (4 or 5) is not an important factor to determine the stability. The differences are significantly larger than those for the divalent oxidation state in [MCl$_2$(bpy)$_2$]$^{n+}$ (M; ΔE = Os, 1.42 V[52]; Re, 1.23 V[3]). Coordination of a stronger π-back-donating ligand such as bpy would stabilize lower oxidation states in these cases.

Electronic Spectra. Figure 6 shows electronic spectra of the complexes [**1a**]BF$_4$, [**2**]PF$_6$, and [**3**]BF$_4$. Numerical spectral data of these complexes as well as those of [**1**]BF$_4$ and [**3a**]BF$_4$ are summarized in Table 4. The most notable difference in the visible region is that fairly strong absorption bands with the extinction coefficient (ε) > 5000 mol dm^3 cm^{-1} are observed only for the rhenium(III) complexes. Similar strong visible bands with $\varepsilon > 10^3$ mol dm^3 cm^{-1} are observed in other rhenium(III) complexes containing pyridine or pyridyl ligands. Seven coordinate rhenium(III) complexes, [ReCl$_2$(qpy)]$^+$ (570 nm (ε = 10010 mol dm^3 cm^{-1})), [Re (terpy)$_2$ (^{t}BuNC)]$^{3+}$ (474 nm (ε, 5860)), and [ReCl(terpy)$_2$]$^{2+}$ (498 nm (ε, 13100)) also show strong visible bands.[3] These strong bands are likely of MLCT character between rhenium and pyridyl ligands. Strong bands are also seen in the μ-oxo-dirhenium(III) complexes of bpy, phen, and tpa.[26] In this case, however, the charge transfer involving an oxide bridge would also be possible. On the contrary to the case of the rhenium(III) complexes, CT bands in visible region are not observed for the ruthenium(III) and osmium(III) complexes, [**1**]BF$_4$, [**1a**]BF$_4$, and [**2**]PF$_6$. In general, the d-orbital energy decreases with increasing atomic number within the same series of the transition elements. Redox potentials for the M(III/IV) process (M = Os, Re) discussed above are consistent with this view. Thus, the energy of the MLCT (dπ–π* transition) is smaller for the rhenium(III) complex than that for the osmium(III) analog. It is interesting to note here that molybdenum(III) complexes, *cis*-[MoCl$_2$(phen)$_2$]$^+$ and *cis*-[MoCl$_2$(bpy)$_2$]$^+$ show strong visible MLCT bands. In the second transition series, Mo(III) may have higher dπ orbitals and thus the MLCT band has lower transition energy than the Ru(III) complexes.[53]

Conclusion. We have prepared isostructural complexes of trivalent ruthenium, osmium, and rhenium with the ligand tris(2-pyridylmethyl)amine (tpa) from RuCl$_3$•3H$_2$O, OsO$_4$, and [ReOCl$_3$(PPh$_3$)$_2$], respectively. The Metpa analogs of Ru and Re were also prepared. Their X-ray structural analyses showed somewhat longer distances for the Re(III) complex than the other two metal complexes. The redox potentials of the complexes depend significantly on the type of metal centers. The potentials for the M(III/IV) and the M(II/III) couples are in the order Re < Os < Ru, with each difference being ca. 0.5 V. The rhenium tpa complex displayed irreversible Re(III/IV) redox couple due to solvolysis in CH$_3$CN, whereas the Re(III/IV) process is reversible for the Metpa complex as the solvolysis is retarded by the steric hindrance of the methyl group. Strong visible MLCT bands are observed only in the rhenium complexes, indicating the highest d-orbital energies as expected from the redox potentials.

The authors are grateful to Dr. Takahiko Kojima at Kyushu University for his valuable discussion about ruthenium complexes.

Table 4. Electronic Spectral Data of [MCl$_2$(L)]$^{n+}$ (M = Ru, Os and Re) (L = tpa and Metpa)[a) in CH$_3$CN

Complex	λmax, nm (ε, dm^3 mol^{-1} cm^{-1})
[Ru$^{\mathrm{III}}$Cl$_2$ (tpa)]$^+$ (**1**)	436 (1390), 315 (5600), 240 (9820)
[Ru$^{\mathrm{III}}$Cl$_2$ (Metpa)]$^+$ (**1a**)	450 (sh), 312 (5120), 242 (8570)
[Os$^{\mathrm{III}}$Cl$_2$ (tpa)]$^+$ (**2**)	455 (1150), 350 (7930), 327 (7860)
[Re$^{\mathrm{III}}$Cl$_2$ (tpa)]$^+$ (**3**)	503 (6440), 440 (sh), 382 (4750), 290 (sh)
[Re$^{\mathrm{III}}$Cl$_2$ (Metpa)]$^+$ (**3a**)	509 (7240), 449 (6310), 400 (5500), 285 (5060)

a) tpa = tris(2-pyridylmethyl)amine, Metpa = (6-methyl-2-pyridylmethyl)bis(2-pyridylmethyl)amine.

References

1 F. A. Cotton, G. Wilkinson, C. A. Murillo, and M. Bochmann, "Advanced Inorganic Chemistry", 6th ed, Wiley-Interscience (1999).

2 S. D. Orth, J. Barrera, M. Sabat, and D. W. Harman, *Inorg. Chem.*, **32**, 594 (1993).

3 L. E. Helberg, S. D. Orth, M. Sabat, and W. D. Harman, *Inorg. Chem.*, **35**, 5584 (1996).

4 O. Arp and W. Preetz, *Z. Anorg. Allg. Chem.*, **622**, 219 (1996).

5 Y. Sasaki, K. Umakoshi, S. Kimura, C.-E. Oh, M. Yamazaki, and T. Shibahara, *Chem. Lett.*, **1994**, 1185.

6 K. Umakoshi, Y. Tsuruma, C.-E. Oh, A. Takasawa, H. Yasukawa, and Y. Sasaki, *Bull. Chem. Soc. Jpn.*, **72**, 443 (1999).

7 T. Inomata, M. Abe, T. Kondo, K. Umakoshi, K. Uosaki, and Y. Sasaki, *Chem. Lett.*, **1999**, 1097.

8 Y. Sasaki, M. Suzuki, A. Tokiwa, M. Ebihara, T. Yamaguchi, C. Kabuto, and T. Ito, *J. Am. Chem. Soc.*, **110**, 6251 (1988).

9 Y. Sasaki, M. Suzuki, A. Nagasawa, A. Tokiwa, M. Ebihara, T. Yamaguchi, C. Kabuto, T. Ochi, and T. Ito, *Inorg. Chem.*, **30**, 4903 (1991).

10 M. Abe, Y. Sasaki, T. Yamaguchi, and T. Ito, *Bull. Chem. Soc. Jpn.*, **65**, 1585 (1992).

11 H. Kobayashi, N. Uryu, I. Mogi, Y. Sasaki, Y. Ohba, M. Iwaizumi, T. Ochi, A. Ohto, T. Yamaguchi, and T. Ito, *Bull. Pol. Acad. Sci., Chem.*, **42**, 455 (1994).

12 A. Kikuchi, T. Fukumoto, K. Umakoshi, Y. Sasaki, and A. Ichimura, *J. Chem. Soc., Chem. Commun.*, **1995**, 2125.

13 T. Imamura, A. Kishimoto, T. Sumiyoshi, K. Takahashi, T. Fukumoto, and Y. Sasaki, *Bull. Chem. Soc. Jpn.*, **68**, 3365 (1995).

14 Y. Sasaki, *J. Mol. Liq.*, **65/66**, 253 (1995).

15 Y. Sasaki, K. Umakoshi, T. Imamura, A. Kikuchi, and A. Kishimoto, *Pure Appl. Chem.*, **69**, 205 (1997).

16 C. Koshi, K. Umakoshi, and Y. Sasaki, *Chem. Lett.*, **1997**, 1155.

17 M. Valli, S. Miyata, H. Wakita, T. Yamaguchi, A. Kikuchi, K. Umakoshi, T. Imamura, and Y. Sasaki, *Inorg. Chem.*, **36**, 4622 (1997).

18 T. Fukumoto, A. Kikuchi, K. Umakoshi, and Y. Sasaki, *Inorg. Chim. Acta*, **283**, 151 (1998).

19 T. Inomata, K. Umakoshi, and Y. Sasaki, *Electrochem.*, **67**, 427 (1999).

20 M. Abe, A. Sato, T. Inomata, T. Kondo, K. Uosaki, and Y. Sasaki, *J. Chem. Soc., Dalton Trans.*, **2000**, 2693.

21 M. Abe, S. Ye, T. Kondo, K. Uosaki, and Y. Sasaki, *Electrochem.*, **67**, 1162 (1999).

22 M. Abe, T. Kondo, K. Uosaki, and Y. Sasaki, *J. Electroanalchem.*, **473**, 93 (1999).

23 J. F. Ojo, Y. Hasegawa, Y. Sasaki, K. Kunimasa, M. Abe, and N. Ohta, *Inorg. React. Mech.*, in press.

24 Y. Imbe, K. Umakoshi, C. Matsunami, and Y. Sasaki, *Inorg. Chem.*, **34**, 813 (1995).

25 T. Takahira, K. Umakoshi, and Y. Sasaki, unpublished.

26 T. Takahira, K. Umakoshi, and Y. Sasaki, *Chem. Lett.*, **1994**, 1870.

27 H. Sugimoto, M. Kamei, K. Umakoshi, Y. Sasaki, and M. Suzuki, *Inorg. Chem.*, **35**, 7082 (1996).

28 H.-Y. Jin, S. Ikari, K. Kobayashi, K. Umakoshi, H. Sugimoto, Y. Sasaki, and T. Ito, to be submitted.

29 H. Sugimoto and Y. Sasaki, *Chem. Lett.*, **541** (1997).

30 H. Sugimoto and Y. Sasaki, *Chem. Lett.*, **197** (1998).

31 M. Abe, T. Mikami, H. Sugimoto, A. Nagasawa, and Y. Sasaki, *Chem. Lett.*, **1073** (1997).

32 J. M. Botha, K. Umakoshi, Y. Sasaki, and G. J. Lamprecht, *Inorg. Chem.*, **37**, 1609 (1998).

33 T. Kojima, *Chem. Lett.*, **1996**, 121.

34 G. Anderegg and F. Wenk, *Helv. Chim. Acta.*, **50**, 2330 (1967).

35 A. R. Oki, J. Glerup, and D. J. Hodgson, *Inorg. Chem.*, **29**, 2434 (1990).

36 N. P. Johnson, C. J. L. Lock, and G. Wilkinson, *J. Chem. Soc.*, **1964**, 1054 (1964).

37 I. P. Evans, A. Spencer, and G. Willkinson, *J. Chem. Soc., Dalton Trans.*, **1973**, 204.

38 C. M. Che, V. W. W. Yam, and T. C. W. Mak, *J. Am. Chem. Soc.*, **112**, 2284 (1990).

39 M. Yamaguchi, H. Kousaka, and T. Yamagishi, *Chem. Lett.*, **1997**, 769.

40 P. T. Beurskens, G. Admiraal, G. Beurskens, W. P. Bosman, S. Garcia-Granda, R. O. Gould,; J. M. M. Smits, and C. Smykalla, The DIRDIF Program System. Technical Report: Crystallography Laboratory, University of Nijmegen

41 C. Edwards, C. J. Gilmore, S. Mackay, and N. Stewart, CRYSTAN 6.3. A Computer Program for the Solution and Refinement of Crystal Structures. Mac Science: Yokohama, Japan, (1995).

42 TEXSAN. Single Crystal Structure Analysis Package. Molecular Structure Corporation: The Woodlands, TX 77381, USA (1992).

43 Li Xu and Y. Sasaki, *Inorg. Chem. Commun.*, **2**, 121 (1999).

44 Li Xu and Y. Sasaki, *J. Organomet. Chem.*, **585**, 246 (1999).

45 Anal. Calcd for $C_{36}H_{36}N_8Cl_{10}Os_3$: C, 28.71; H, 2.41; N, 7.44%. Found: C, 28.87; H, 2.58; N, 7.45%. FAB MS *m/z* 552 ($[OsCl_2(tpa)]^+$).

46 H. Sugimoto, T. Takahira, T. Yoshimura, K. Umakoshi, H. Miyake, and Y. Sasaki, unpublished results.

47 P. K. Ho, K. Cheung, S. Peng, and C. Che, *J. Chem. Soc., Dalton Trans.*, **1996**, 1411.

48 D. S. Eggleston, K. A. Goldsby, D. J. Hodgson, and T. J. Meyer, *Inorg. Chem.*, **24**, 4573 (1985).

49 C. M. Elson, I. J. Itzkovitch, J. McKenny, and J. A. Page, *Can. J. Chem.*, **53**, 2922 (1975).

50 C. K. Poon, C. M. Che, and Y. P. Kan, *J. Chem. Soc., Dalton Trans.*, **1980**, 128.

51 J. D. Buhr, J. R. Winkler, and H. Taube, *Inorg. Chem.*, **19**, 2416 (1980).

52 G. F. Strouse, J. R. Schoonover, R. Duesing, S. Boyde, W. E. Jr. Jones, and T. J. Meyer, *Inorg. Chem.*, **34**, 473 (1995).

53 T. S. Morita, Y. Sasaki, and K. Saito, *Bull. Chem. Soc. Jpn.*, **54**, 2678 (1981).